The Deformation of Aluminum Foams

P. H. THORNTON AND C. L. MAGEE

The compressive flow behavior of Al, Al-7 pct Mg and 7075 Al alloy foams has been determined in structures whose void fraction varies from 0.80 to 0.95 of the total volume. In all cases, a greater than linear increase in flow strength with increase in density was exhibited, indicating that bending stresses within the foam structure are an important feature of the collapse mode. The flow strength did not follow proportionately changes in bulk flow strength in comparisons of either alloy or of heat-treatment conditions. Ancillary tensile and metallographic observations show that this lack of correlation arises because the different foams collapse by different modes with localized fracture becoming dominant in the higher strength 7075 alloy.

The energy absorbing efficiency was found to be independent of foam density for all the materials. However, the efficiency was found to be a strong function of the alloy and heat treatment increasing from about 30 pct in Al, to 43 pct in Al-7 pct Mg and to 50 pct in the solution heat treated and aged 7075 alloy. The increase in efficiency occurs because of an increase in the propensity to fracture in the higher strength alloys which introduces the potential for a propagating constant-stress collapse process.

THE presence of a few percent of voids in a solid material is a well-known result of solidification and powder metallurgy processing techniques. Investigations of the (almost always) deleterious effects of these voids have proceeded on theoretical and experimental bases and much work has naturally been focussed on finding means for eliminating the porosity.[1] This paper is concerned with solids where a different extreme in porosity is purposefully present. Aluminum base foams have been known for some time[2] and are best characterized as solid aluminum alloys containing greater than about 50 volume pct voids. The aim of the various processing techniques is to obtain a uniform high porosity in a solid structure. By analogy with the related cellular forms of rigid polymeric materials,[3] the major potential applications are in the stiffening of low weight structures, *e.g.* sandwich panels, and in energy absorbing or cushioning applications.

The purpose of the present work was to investigate the influence of several metallurgical parameters on the energy-absorbing characteristics of Al base foams. The parameters include alloy composition, heat treatment and foam density. Many of the polymeric foam systems have been well characterized[4,5] but there are no previous systematic studies of metallic foams. Theoretical models which have been employed for interpreting the load deformation response of foams generally are limited to a buckling analysis of a specific geometrical structure[6-11] and do not consider other deformation phenomena or the reasons for the various shapes of the stress-strain curves for different foam materials. Several advantages in studying aluminum rather than polymeric foams should also be noted. For example, changes in the bulk material properties can be made by heat treatment without concommitant changes in the elastic modulus. In addition, the collapse mode can be determined directly by a metallographic technique.

For the purposes of the work reported here, it is important to recognize that several energy-absorption parameters are wholly determined by the conventional deformation response. First, the energy absorbed per unit volume is simply the area under the stress-strain curve. A second parameter of interest is the energy-absorbing efficiency since one desires to transmit the minimum possible force to a body possessing a given kinetic energy. The efficiency, E, is defined by

$$E = \frac{\int_0^l F \cdot dl}{F_{\max} L} \qquad [1]$$

where the numerator is the actual energy absorbed after deformation over the collapse distance l and the denominator is the "ideal" energy absorption, given by the product of the maximum force applied over the collapse distance l, $F_{\max}$, and the sample length L. For all real materials or devices $F_{\max}$ depends on the degree of deformation so the calculated efficiency depends on the particular values of the stress and strain used for calculation. As will be seen later, the efficiency usually reaches a maximum at some intermediate strain and this maximum efficiency is the important parameter for design considerations. The essential point for this report is that the shape of the stress-strain curve wholly determines the efficiency.

I. EXPERIMENTAL PROCEDURES

Foam samples* of Al, Al-7 pct Mg, and 7075 alloy were supplied in the form of bricks approximately 12 in. × 6 in. × 5 in. (0.3 m × 0.15 m × 0.13 m) with nominal densities in the range 8 to 35 lbs/ft^3 (200 to 500 kg/m^3).

*The materials were kindly supplied by the Ethyl Corp., Baton Rouge, La.

In addition to the normal alloying additions and impurities, these materials contained approximately 1 pct Zr as a residue from the foaming agent. Because of the foaming and casting technique, the blocks almost invariably exhibited density gradients. The average density was determined on *each* specimen machined from the brick prior to mechanical testing. Compression tests were performed on an Instron at strain rates of up to 10^{-1} s^{-1}. Samples were tested primarily in the as re-

P. H. THORNTON and C. L. MAGEE are with Scientific Research Staff, Ford Motor Company, P. O. Box 2053, Dearborn, Mich. 48121.

Manuscript submitted July 19, 1974.

Table I. Solution and Aging Heat Treatments

Foam	Treatment	
Al–7 pct Mg	Solution *H/T*	2 h/840°F (449°C)
	Age	1 h/180°F (82°C)
		8 h/200°F (93°C)
7075	Solution *H/T*	1 h/900°F (482°C)
	Age	24 h/120°F (49°C)

ceived or "as cast" condition. The Al-7 pct Mg and 7075 alloys were also tested after solution treating and aging heat treatments, as shown in Table I.

The foam samples were examined by conventional light microscopy. In order to preserve the foam structure during the polishing operations, a self-curing plastic mixture ("Araldite") was first injected into the foam. Typical low-magnification micrographs are shown in Fig. 1. The cell sizes determined from such

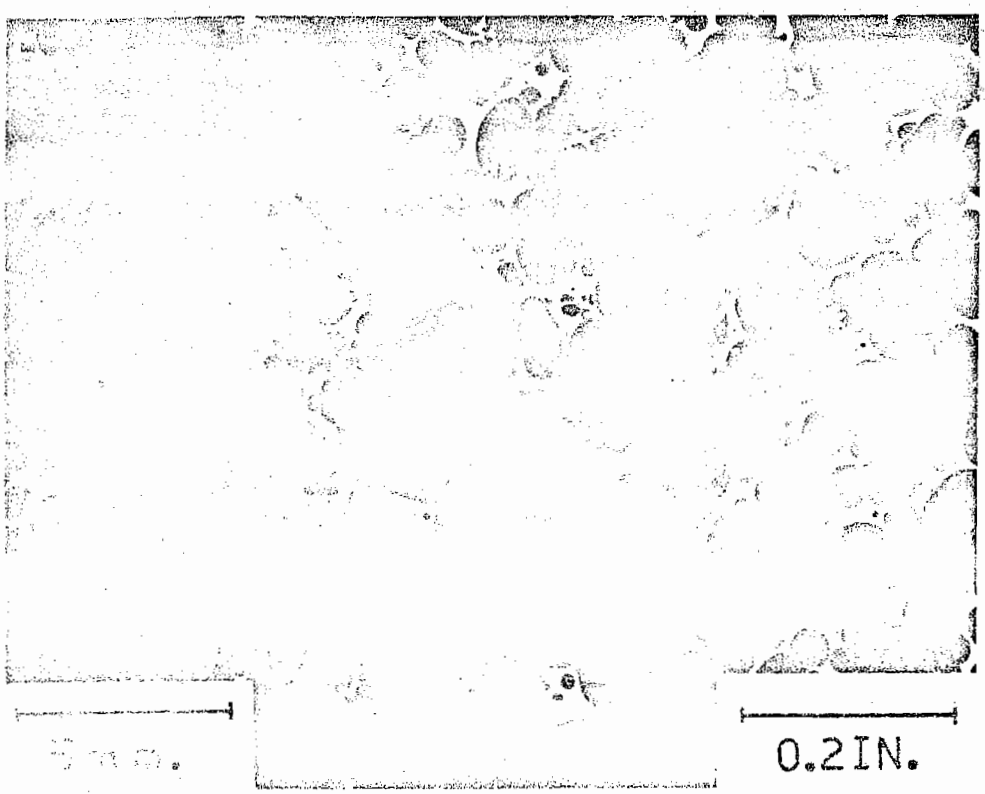

(a)

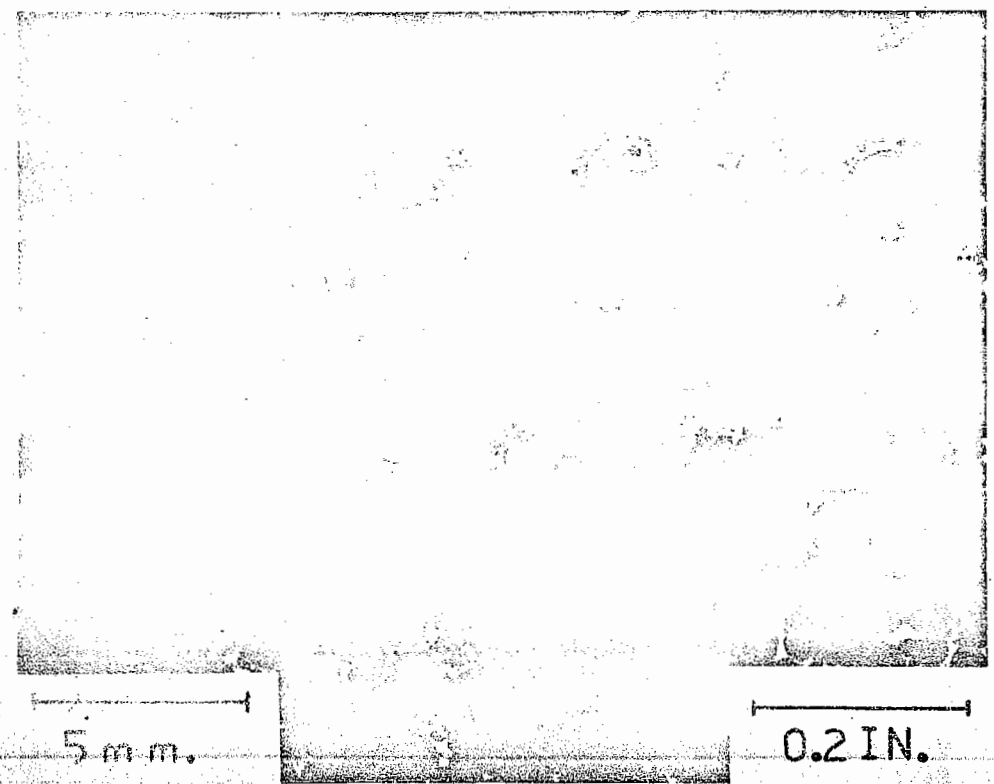

(b)

Fig. 1—(*a*) Structure of aluminum alloy foams; (*a*) aluminum foam, density ratio ρ 0.12; (*b*) 7075 alloy foam, density ratio ρ 0.11; (*c*) Al-7 pct Mg alloy foam, density ratio ρ 0.12.

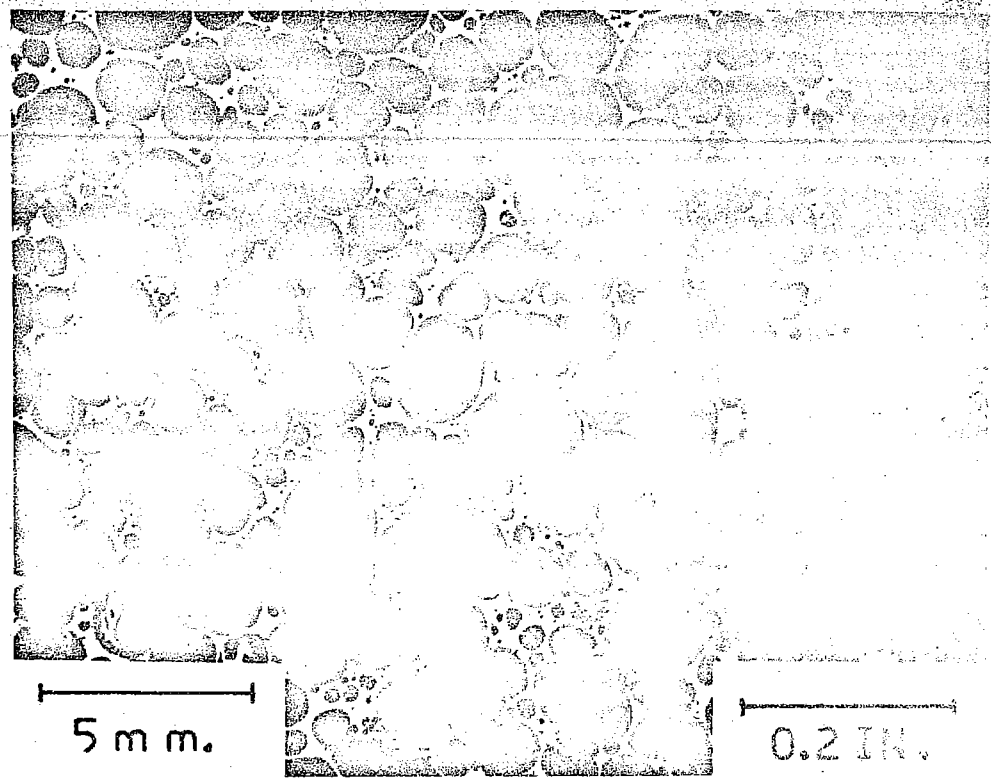

Fig. 1—Continued

Table II. Cell Size Distributions

Foam	Density Ratio	Mean Cell Size In. (mm)
Al	0.056	0.081 (2.06)
	0.145	0.048 (1.22)
Al – 7 pct Mg	0.069	0.101 (2.56)
	0.184	0.042 (1.06)
7075	0.057	0.075 (1.91)
	0.187	0.235 (5.98)

micrographs are given for various alloys and nominal densities in Table II. Higher magnification examination revealed no important structural differences as all alloys showed some small internal porosity and inclusions.

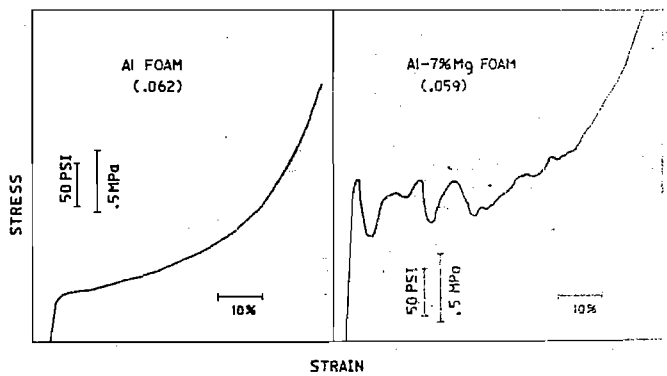

Fig. 2—Flow stress curves for as-cast Al and Al-7 pct Mg foam.

II. RESULTS

In this section, compression results for each alloy will be considered first and then ancillary results concerning collapse mode determinations, bulk properties and tensile results on some foams will be presented.

A) Compression

1) As-cast foams. Typical compression curves for an Al foam and an Al-7 pct Mg foam are shown in Fig. 2. The Al foam deformed smoothly throughout the entire flow range, *i.e.*, up to ~75 pct strain. In contrast the flow stress curve for Al-7 pct Mg shows marked serrations, particularly at the onset of plastic flow when pronounced upper and lower yield points were often observed. Serrated flow was particularly marked in the case of the 7075 alloy. When serrated flow was observed, flow stresses were determined by extrapolating through the initial yield transient a best average line based upon the peak loads. This technique has been found to give consistent results for the determination of flow stresses in the case of the formation of martensite during the plastic deformation of austenite.[12] Measurements were made also of the upper and lower yield points in order to obtain the range of stresses over which plastic deformation would occur.

Figs. 3, 4 and 5 show the flow stress, L.Y.P. and U.Y.P. as a function of density for the Al, Al-7 pct Mg and 7075 foams. Over the comparable ranges of densities the flow stress for the Al foam was always much less than that for the two alloy foams. In addition, the results for the Al-7 pct Mg and 7075 foams showed much more scatter than did those for the Al foam. whichever parameter, flow stress, L.Y.P. or U.Y.P. was used as a criterion for the onset of plastic deformation and there was a much greater difference between the parameters in the case of the 7075 foam than for the Al-7 pct Mg foam. Both of these effects are a consequence of the serrations observed in the

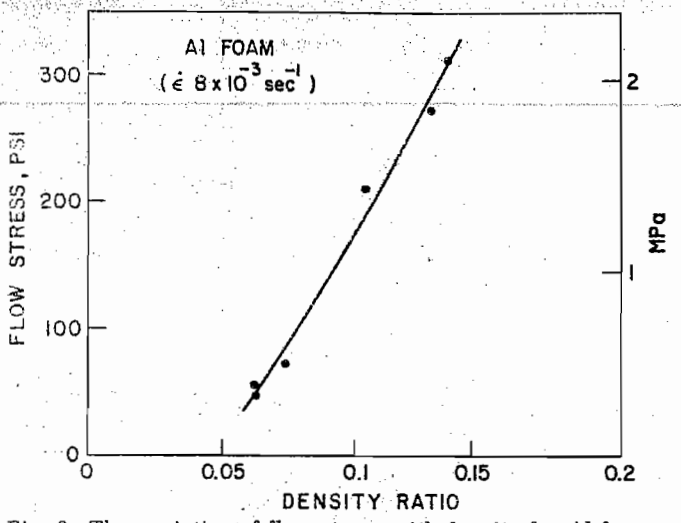

Fig. 3—The variation of flow stress with density for Al foam.

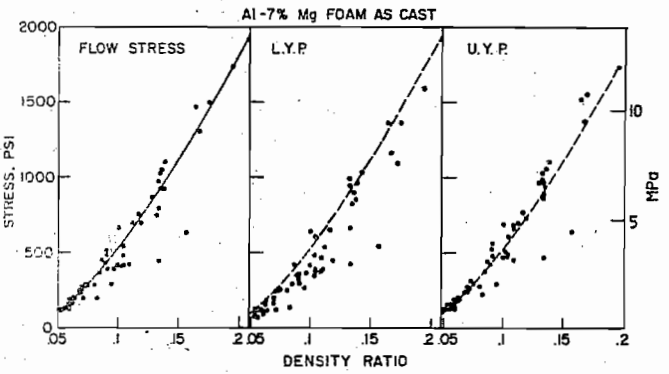

Fig. 4—The variation of flow stress, U.Y.P. and L.Y.P. with density for as-cast Al-7 pct Mg foam.

flow stress curves for the alloys.

The results in Figs. 3, 4 and 5 illuminate a discrepancy between the mechanical response of the foams and the bulk alloys. Over the comparable range of densities, the Al-7 pct Mg foam is stronger than the 7075 foam; the bulk 7075 alloy however is considerably stronger than the bulk Al-7 pct Mg alloy, the yield stresses being approximately 50,000 psi (344 MPa) and 30,000 psi (206 MPa) respectively. This discrepancy between trends in the mechanical properties of the foams and the bulk alloys is greatest at the lowest densities.

2) Effect of Heat Treatment. The yield stress of the 7075 alloy can be markedly affected by heat treatment and such alterations in the characteristics of the bulk alloy offer a useful tool for examining changes in the properties of the foam. Fink and Smith[13] have demonstrated that Al-Mg alloys are susceptible to aging treatment, although the strength increases are small and are accompanied by marked embrittling effects. Results from the present study are shown in Table III for bulk material properties. Samples of both alloy foams were tested in either the solution heat treated or solution heat treated and aged conditions. Although the flow stress of the solution treated and aged Al-7 pct Mg alloy in the bulk form was dependent upon the aging treatment employed, the changes produced were small, Table III. In the case of the foam, no differences were observed in the properties generated by

Table III. Mechanical Properties of Alloys

Alloy	Condition	0.1 pct Flow Stress psi (MPa)
Al	Cast	7600 (52.2)
Al – 7 pct Mg	Cast	33,300 (229)
	Solution Treated	29,700 (204)
	S/T, aged 1 h/180°F (83°C)	28,900 (199)
	S/T, aged 8 h/200°F (93°C)	30,900 (212)
7075	Cast	49,640 (342)
	Solution treated	40,000 (275)
	S/T, aged	73,000 (502)

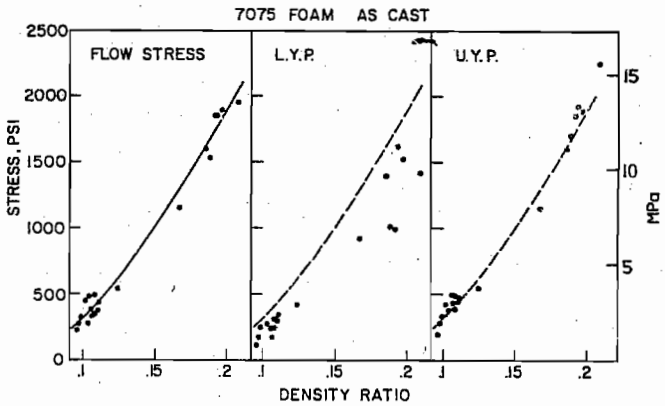

Fig. 5—The variation of flow stress, U.Y.P. and L.Y.P. with density for as-cast 7075 alloy foam.

the two aging treatments, perhaps due to the scatter in the results. Hence in this work the two aging treatments are not distinguished. Fig. 6 shows the flow stress curves in the three conditions of interest for 7075 foam. In the solution treated samples, the magnitudes of the initial yield drop and of the load oscillations during serrated flow were substantially reduced as compared to "as cast" samples. An aging treatment, after solution heat treating, restored the initial load drop, but the subsequent plastic flow, although serrated, occurred at a more constant level over a wider range of deformation.

The yield stress parameters of the foams as a function of density are presented in Figs. 7 and 8 for the Al-7 pct Mg and 7075 alloys respectively. Other than to reduce the scatter in the results there was little apparent effect of heat treatment upon the magnitude of any of these parameters in the case of the Al-7 pct Mg foam. The major effect of heat treatment in this case was to make the flow stress curves much smoother. The U.Y.P. and L.Y.P. of the 7075 alloy foam are raised by solution heat treatment and aging heat treatments, Figs. 5 and 8. However, the effect is not as large as the changes in bulk properties produced by similar heat treatments, Table III.

B) Collapse Mechanism

In addition to the quantitative results in the preceding section, other observations were made during the compression tests. For all alloys in all conditions, the initial collapse occurred without significant change in the lateral dimensions so the volume of the sample

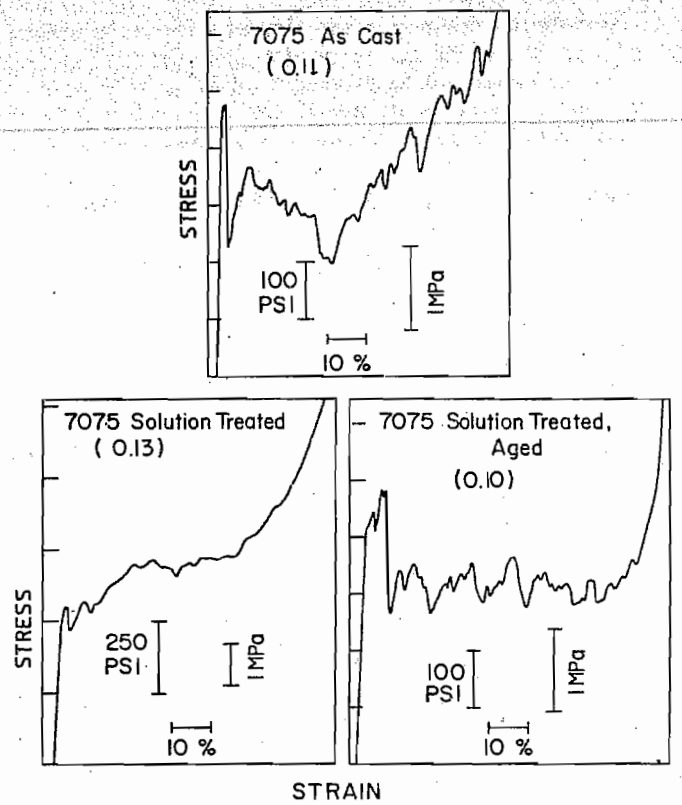

Fig. 6—The effect of heat treatment on the stress-strain curves for 7075 alloy foam.

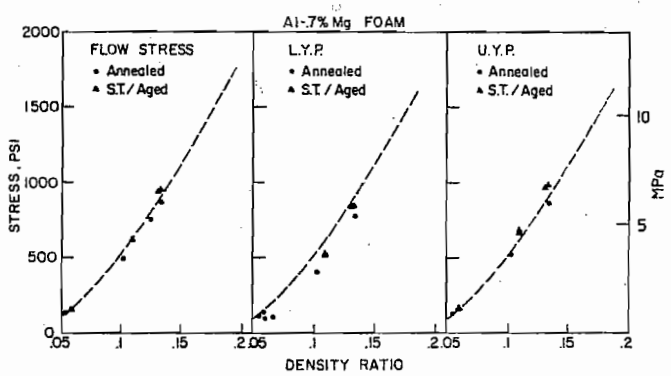

Fig. 7—The variation of flow stress, U.Y.P. and L.Y.P. with density for heat treated Al-7 pct Mg foam. The dash line is the flow stress/density curve for as-cast material (Fig. 4).

decreased by a factor of approximately 2 with 50 pct deformation.* At higher strains, the Al foam samples showed some lateral expansion whereas the alloy samples tended to crumble, indicating that in these samples local fracture was occurring during compression. As cast Al-7 pct Mg foam samples, whose height was greater than about twice the lateral dimensions, were found to fail by large-scale shear across the section during compression. After solution treatment and aging the alloys tended to crumble into small pieces during compression. Both of these observations correlate with the deformation response noted previously in that large serrations were associated with the tendency towards unstable local fracture.

Metallographic study of compressed foams has

*This is consistent with the reduction of Poisson's ratio found in porous solids formed from compacted powders.[1]

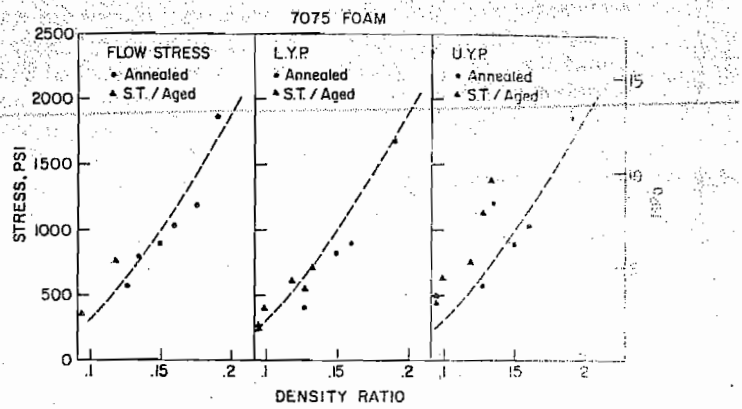

Fig. 8—The variation of flow stress, U.Y.P. and L.Y.P. density for heat treated 7075 alloy foam. The dash line is the flow stress/density curve for as-cast material (Fig. 5).

shown the structural collapse modes more clearly. Macrophotographs of Al and 7075 alloy foam specimens, after deformation to various strains in the range 10 to 70 pct are shown in Figs. 9 and 10 respectively. These materials represented the extremes of behavior observed. In the Al foam, structural collapse occurred mostly by buckling of the cell walls throughout the entire deformation range and the buckling appeared to be uniformly distributed over the whole sample even at the lowest strains, Fig. 9. In contrast the 7075 foam collapsed by fracture of the cell walls, and no buckling modes were discerned. Total failure, *i.e.* essentially complete compaction, occurred locally and spread to the surrounding regions as the compression proceeded, in a manner analogous to Luders band propagation. Even after 70 pct deformation there were still cell regions in the 7075 alloy which appeared to be in the original undeformed state, Fig. 10.

Further evidence of the difference in fracture behavior for the various alloys is given in Fig. 11 where tensile results are plotted for the Al and Al-7 pct Mg foams. The samples now all fail by localized fracture, and except for the very low density Al foams, the flow stress in tension is less than that in compression for a given density of foam.

These results indicate certain practical limits to the use of the foams but more importantly for the present purpose provide important evidence for the interpretation of the differences in the collapse curves. Before considering this aspect of the deformation response of the foams the implications of these results in terms of energy absorption will be considered.

C) Energy Absorption

The energy necessary to deform specimens either 25 pct, 50 pct or 75 pct was calculated from the area under the load-deflection curve for alloys in various heat treatment conditions and densities and the results are shown for the three alloys in Figs. 12 thru 14. Since these results are directly related to the average flow stress, the results show trends similar to those in Figs. 3 thru 8. Again, the results do not correlate with bulk flow stress (compare Al-7 pct Mg with heat-treated 7075 alloy—Table III and Figs. 13 and 14).

As noted in the beginning of the article, the energy

absorbing capacity is only one parameter of interest. The energy absorbing efficiency (as defined in Eq. [1]) is shown in Fig. 15 as a function of the compressive strain for several of the foams. In all cases a peak in the efficiency occurs at some intermediate strain due to a relatively rapid increase in the work hardening rate (thus the denominator in Eq. [1] increases more rapidly than the numerator). The peaks are clearly much broader for the Al foam than for the alloy foams reflecting the more gradual change in work hardening rate for the Al, see Figs. 2 and 6. The most important practical parameter for comparing materials is the peak efficiency and this is shown in Fig. 16 as a function of relative density. The results exhibit considerable scatter but two important findings emerge. The first is that the relative density has no discernable effect on efficiency in any of the alloys. Secondly, there is an increase in efficiency in the foam composition sequence Al, Al-7 pct Mg and 7075 alloy. These quantitative results follow the qualitative trend towards

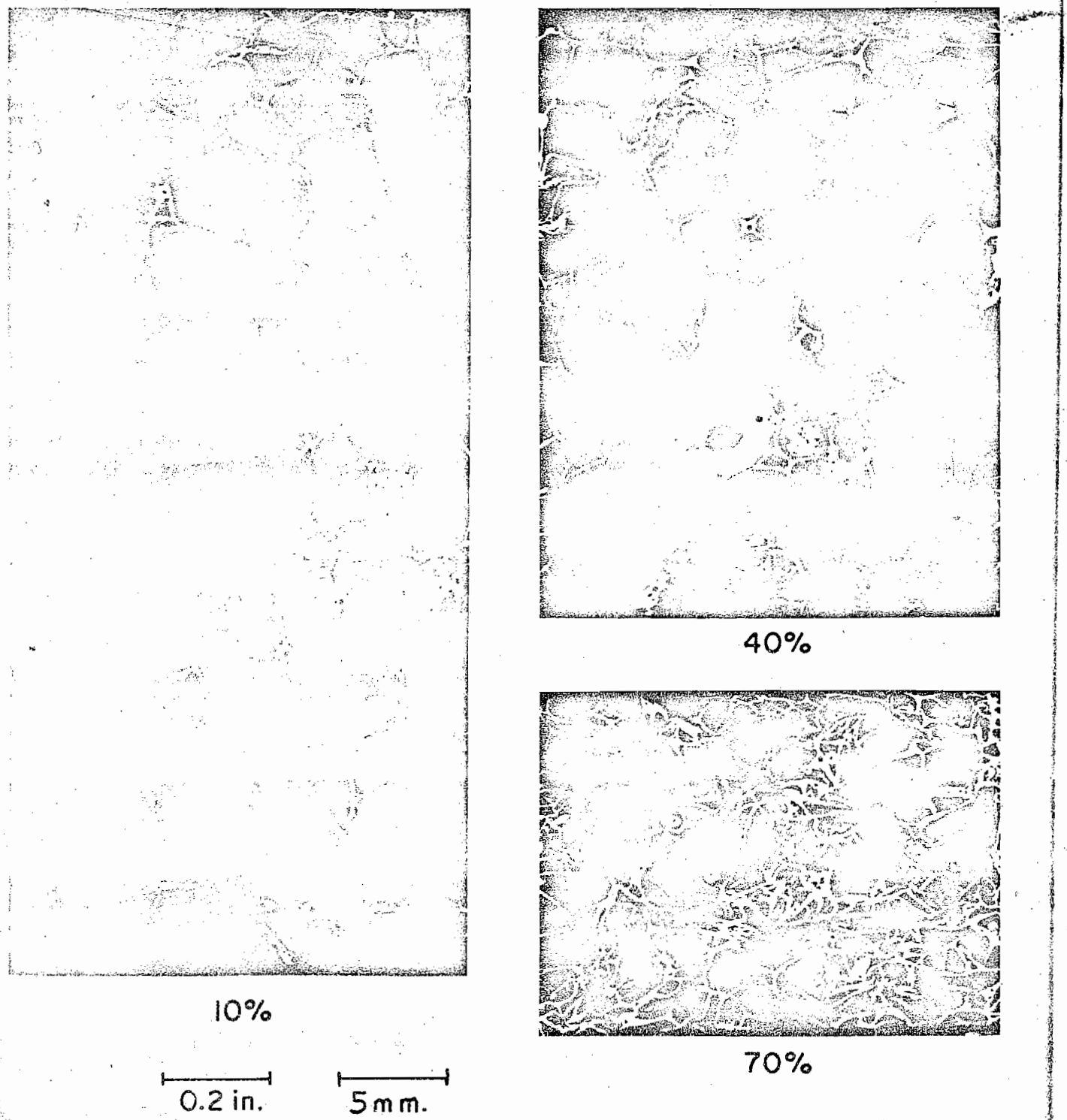

Fig. 9—The structure of Al foam samples after compressions of 10 pct, 40 pct and 70 pct.

flatter stress-strain curves through the same series of materials. Thus, we reemphasize that the energy-absorbing efficiency is a function of only the shape of the stress-strain curve.

DISCUSSION

A) Collapse Models

Several models have been suggested to explain the flow strength of polymer foams.[6-11] All treat the constrained buckling in the cell walls or edges and predict that the flow strength depends on the elastic modulus; they differ only in how the constraints of foam structure on buckling are treated. The present results show several discrepancies with respect to these models. First, the flow stress for the aluminum foams predicted from the models is at least an order of magnitude higher than the experimental results. Second, the models do not easily account for the difference in strength of the various alloy foams for a given density

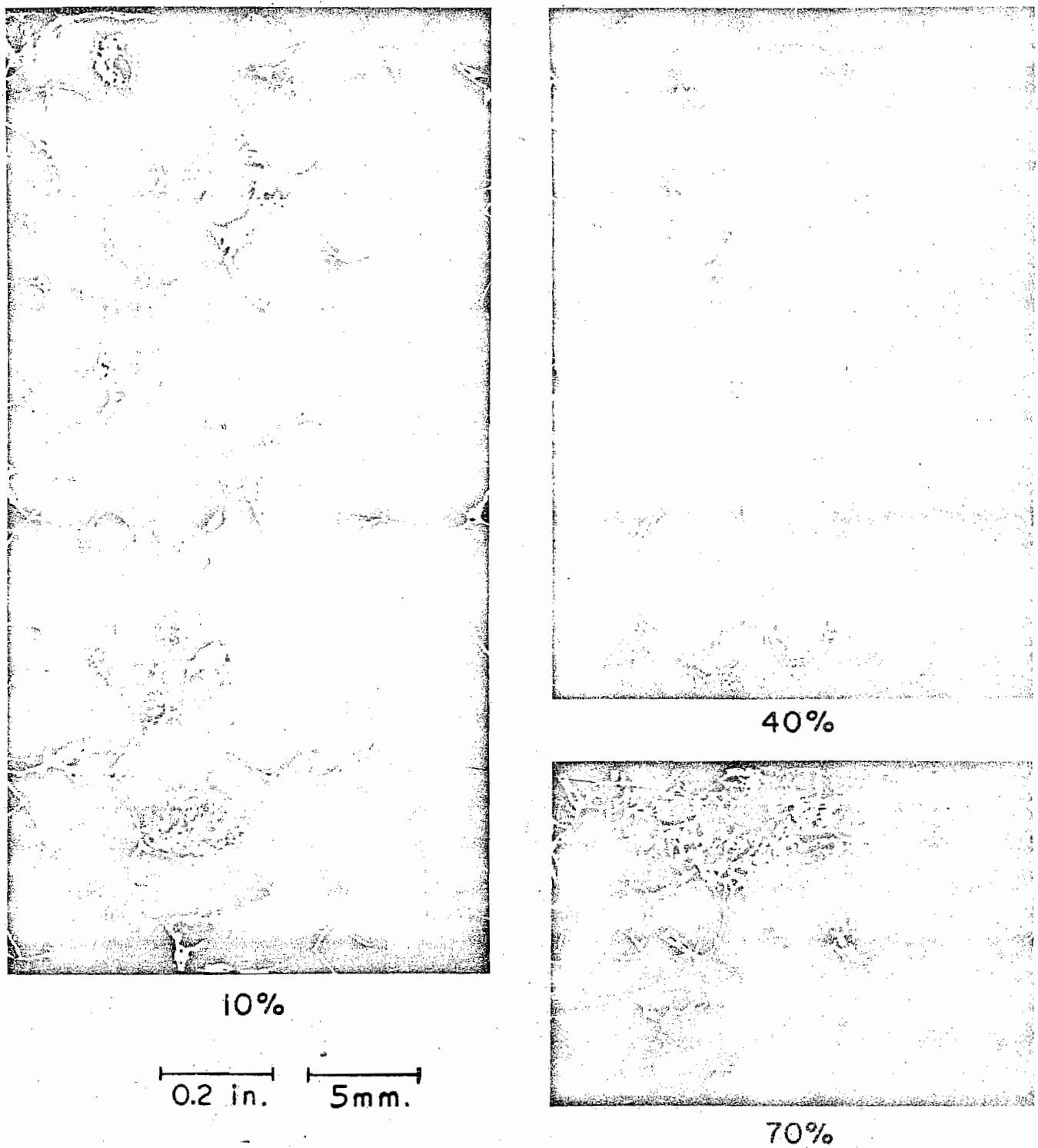

Fig. 10—The structure of 7075 foam samples after compressions of 10 pct, 40 pct and 70 pct.

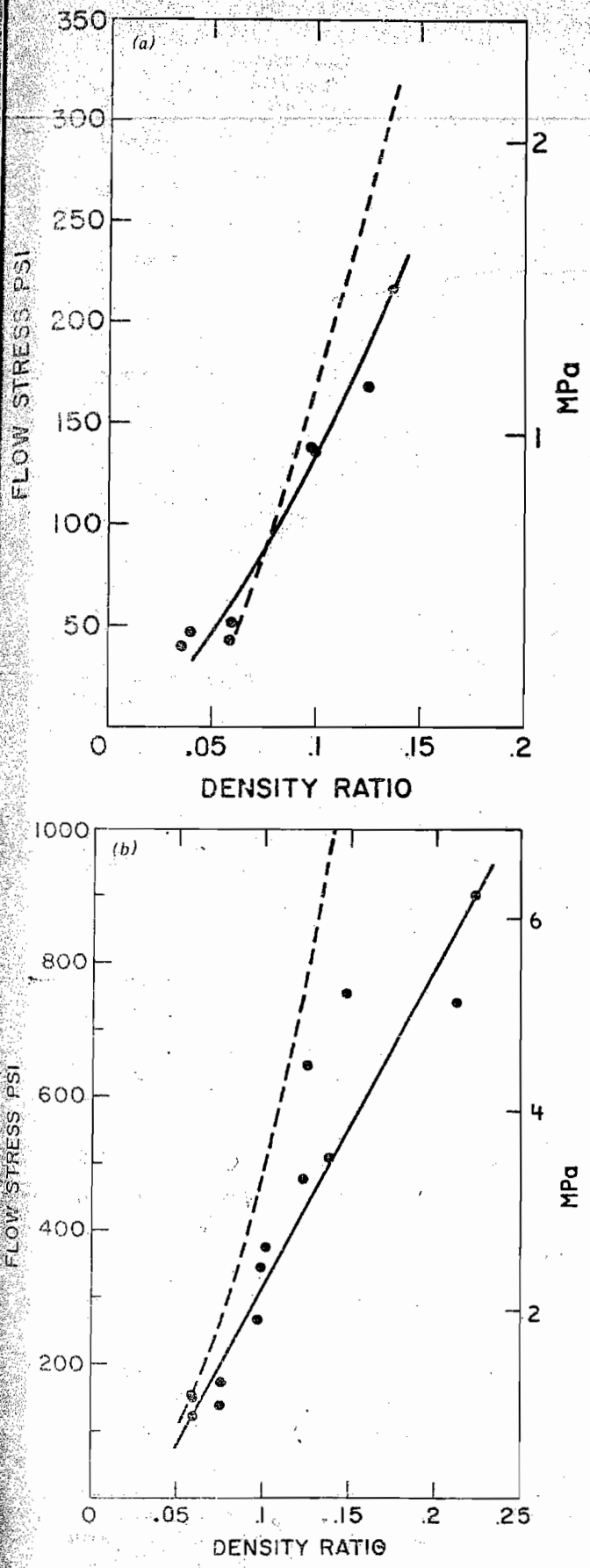

Fig. 11—(*a*) Tensile strength of as-cast Al foam as a function of density; (*b*) tensile strength of as-cast Al-7 pct Mg foam as a function of density. In both (*a*) and (*b*) the flow stress in compression as a function of density is shown as a dashed line.

since the elastic moduli do not differ significantly. Third, the models predict higher flow stresses for tension than for compression in contrast to our results, see Fig. 11.

The failure of the available models to explain the present result is thought to arise from the neglect of the several different mechanisms of collapse for the foams. Since the foams can collapse by a variety of mechanisms, the one which occurs in a given foam is the *easiest* one in that case. We consider two simple (hypothetical) collapse mechanisms as an example. In both of these, the detailed structure and constraints are neglected and the foam structure is modelled by a cube array as shown in Fig. 17.

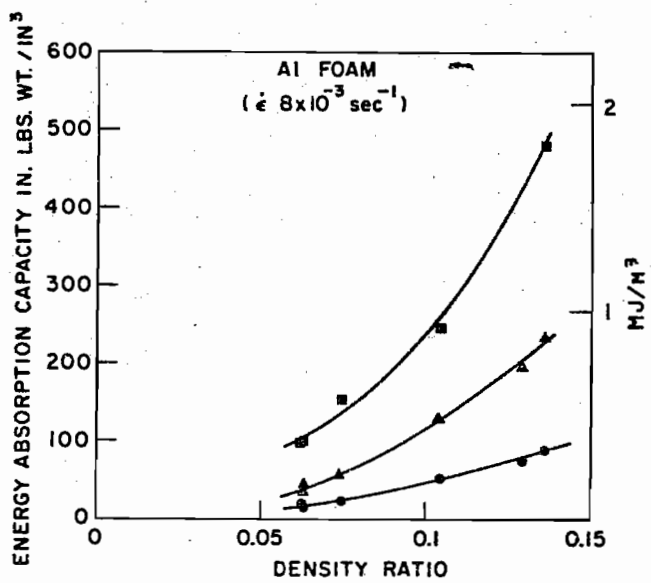

Fig. 12—The variation of the energy absorption capacity of Al-7 pct Mg foam in various heat treatment conditions with change in density.

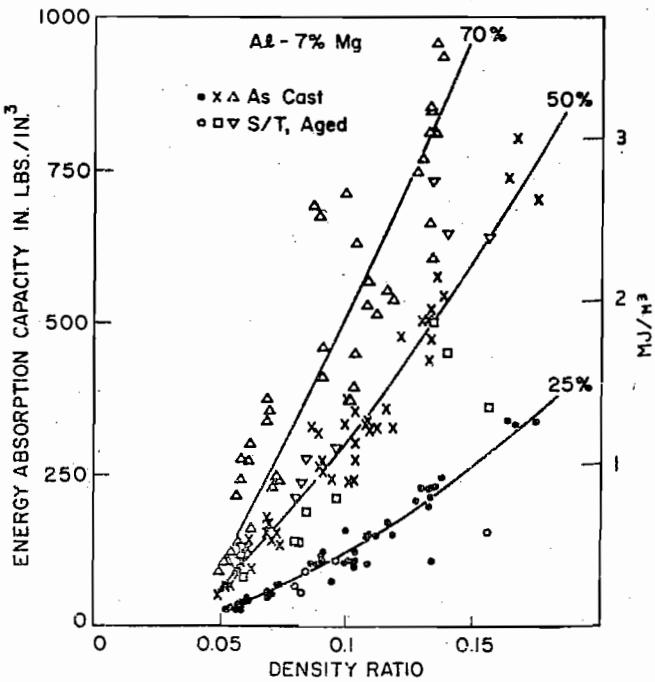

Fig. 13—The variation of the energy absorption capacity of Al-7 pct Mg foam in various heat treatment conditions with change in density.

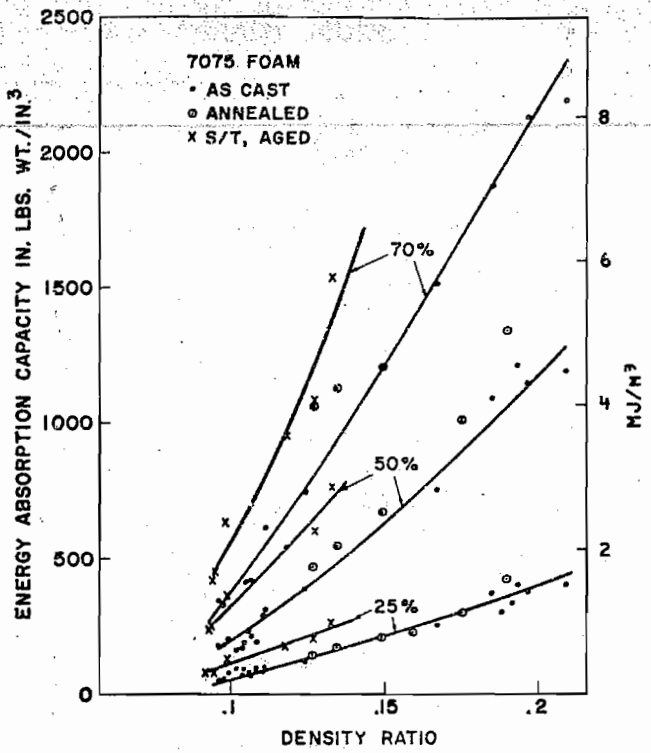

Fig. 14—The variation of the energy absorption capacity of 7075 alloy foam in various heat treatment conditions with change in density.

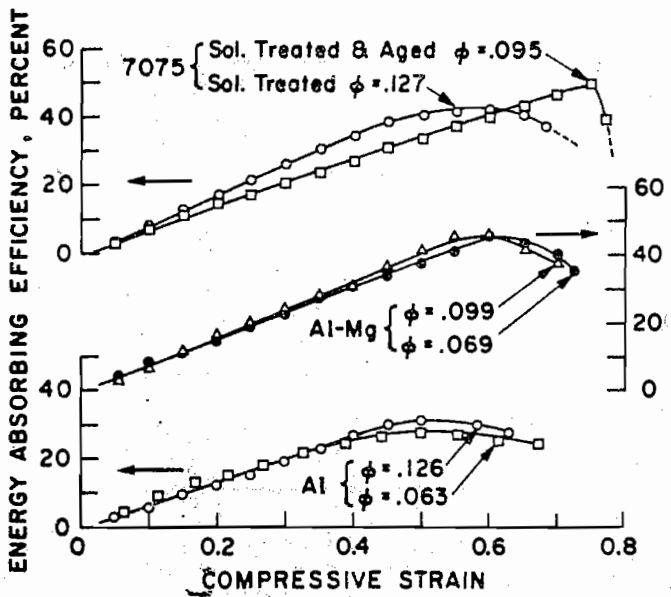

Fig. 15—The energy absorption efficiency of Al, Al-7 pct Mg and 7075 alloy foam as a function of the compression strain.

i) The simplest mechanism of collapse occurs when each cell wall undergoes uniform compression. In this case, the force to collapse one wall is

$$F = \sigma \cdot tl \qquad [2]$$

where σ is the bulk compressive flow strength, t the wall thickness and l the wall length. The collapse stress of the foam, σ_f, is given by the product of F and the number of cell walls per unit area, N_w; for the cube array, N_w is simply given by

$$N_w = 1/l^2 \qquad [3]$$

and thus

$$\sigma_f = \sigma t/l \equiv \sigma\varphi$$

where φ is the density of the foam relative to that of the bulk alloy. This simple mechanism predicts that the strength of the foam is linearly proportional to the density, which is not in agreement with the present results (Figs. 3 thru 8).

ii) For the case where collapse occurs due to the bending of preformed hinges at cell edges (Fig. 17(b)), the load to bend a single hinge is[15]

$$F_h = 2\,\frac{\sigma t^2 l}{6}\,\frac{1}{L} \qquad [4]$$

where L is the lever arm ($l/2$ for simple case in Fig. 17). The flow stress is now the product of F_h and the number of hinges per unit area, N_h, where N_h is proportional to $1/l^2$. For compatible collapse, at least 3 hinges are needed for each cell wall. If $N_h = 3/l^2$, the flow stress of the foam is given by

$$\sigma_f = 2\sigma\,\frac{t^2}{l^2} \equiv 2\sigma\varphi^2. \qquad [5]$$

Although the predictions from this model are in fair agreement with the results for the Al foam, the oversimplifications employed for both the structure and collapse mode render this agreement merely nominal. However, the hinge collapse mode predicts the higher than linear dependence on relative density found in most of our results.

More reasonable deformation collapse models would involve combinations of the above two cases in order to define properly the collapse process in the actual three dimensional structures. However, none of these would be sufficient to treat the results for the Al-7 pct Mg and 7075 alloy foams because all such combinations

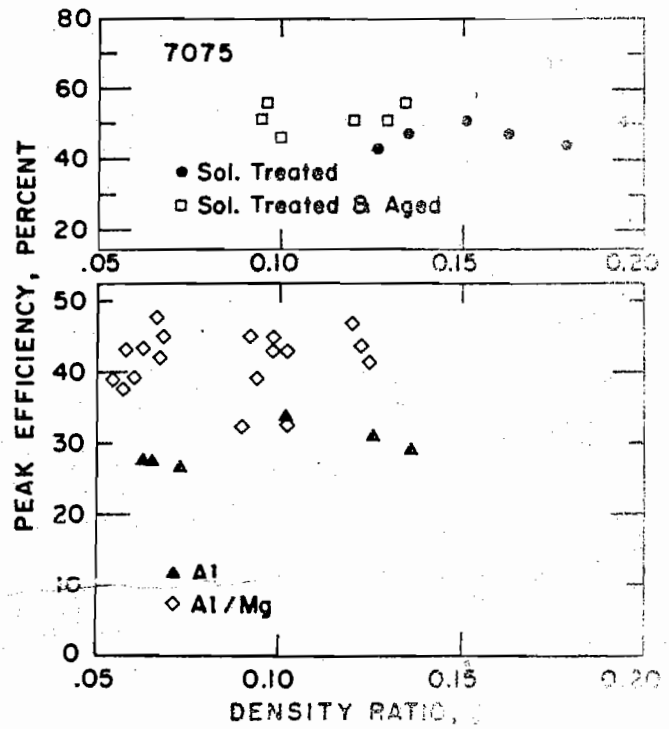

Fig. 16—Peak efficiency *vs* relative density for the Al, Al-7 pct Mg and 7075 alloy foams.

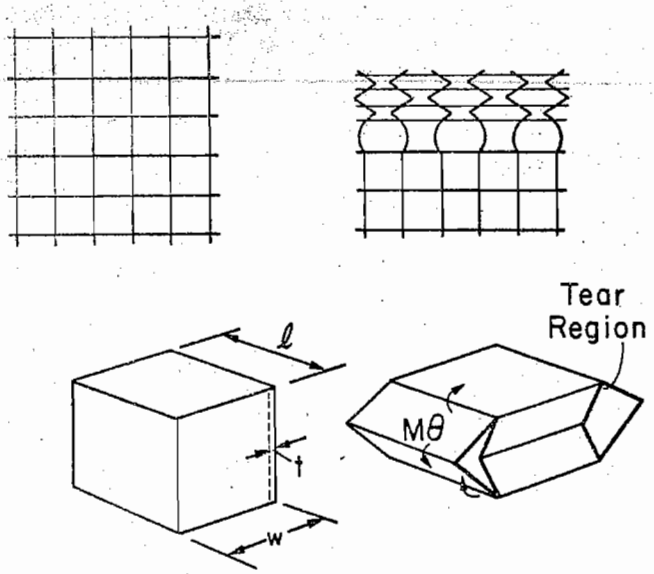

Fig. 17—Model simple-cube foam structure.

predict that the flow stress of a foam is proportional to the bulk flow strength. Our results clearly demonstrate the opposite, *i.e.*, that foam flow stresses are not proportional to bulk flow strengths. In addition, the collapse mode observations reveal that in the alloy foams, deformation is not the only collapse mode since fracture becomes important (Al-7 pct Mg) and then dominant (7075 alloy) at higher bulk flow strengths. Thus, collapse mechanisms involving local fracture must be treated. When this is done, the foam flow strength becomes proportional to the fracture *stress* and *strain* (instead of flow strength). Quantitative comparisons of experimental results with such models are not feasible due to the difficulty in reliably measuring the fracture parameters in truly comparable as-cast structures. However, the basic qualitative trends in foam flow strength are consistent with the reasonable expectation of reduced fracture resistance in the higher strength alloys. It should therefore, be recognized that mechanical properties of a foamed material will not have a unique relationship to specific bulk properties but instead that the relationship will depend on the operative collapse mechanism. Thus, the material properties have a two-fold effect on the properties of a foam. First, the properties (along with structure) determine the collapse mode. Secondly, for a given collapse mode the bulk material properties enter directly (again with structure) to determine the collapse loads. A schematic representation of these effects are shown in Fig. 18.

B) Energy-absorbing Efficiency

The differences in energy-absorbing efficiency noted for the various alloys can also be rationalized on the basis of the different collapse mechanisms which operate. The key to high energy absorbing efficiency is to have large-strain deformation processes occur at the same load level in various parts of the structure.

Although the controlling event ideally will not vary with position in the foam, in practice the specimen-

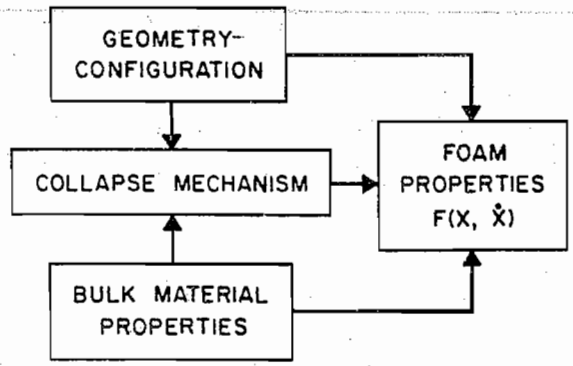

Fig. 18—Interaction of structural and material parameters in the establishment of the foam properties.

platen interface provides the weak link where the collapse process can be initiated. At this interface the cell walls receive their mutual support from one side only, so that the structure in this region tends to be intrinsically weaker than that in the interior. If the bulk material is malleable, the cell walls will buckle, and by analogy with the edge-wise collapse of a plate,[16] will continue to support an increasing load until collapse is initiated in another region in the specimen, which may be in the interior. The Al foam thus collapses by inhomogeneous deformation in randomly dispersed local regions, with a trend for continuing collapse to occur at an increasing stress. However, if the collapse mode involves fracture, the collapse zone generates a new free surface at which further collapse can start. Hence in brittle foams, deformation of the specimen usually occurs by progressive collapse from a free surface into the interior of the specimen. Since subsequent deformation events are closely similar, one expects a flat stress-strain curve in this case. The analogy of the results in Fig. 10 to Luders band propagation (at almost constant stress) is again useful.

The interaction of structural and material characteristics which determines the foam properties, Fig. 18, is highlighted by the tensile results on these metal foams, Fig. 11. The present results appear to be in direct contrast to the response of polymer foams, in which the tensile flow stress apparently always exceeds the compressive flow stress.[10,14] For flexible polymer foams, this difference is very large, but is greatly diminished with an increase in rigidity of the foam. However, these reported results have only considered one particular density in each case, and as can be seen in Fig. 11, the observed flow stress difference between tension and compression depends upon the density of the foam. In particular, as plastic deformation, rather than fracture, tends to dominate the collapse process in the foam structure, so the tensile stress tends to increase relative to the compressive flow stress.

CONCLUDING REMARKS

The results presented here have some implications to the potential application of foamed metals. The ten-

sile results show that particularly for the higher strength alloys the foams cannot be used in situations where tensile stresses operate—*e.g.*, bending. In compression, we found the energy absorbing capacity to increase more rapidly than linearly with density increases so the specific energy absorption capacity (energy absorbed per unit weight) increases with density. Since the energy absorbing efficiency was independent of density, the results indicate that more effective designs are possible with the higher density foams. A comparison of the behavior of the various alloys studied also indicates that a compromise between the tensile properties and the energy absorbing efficiency in compression must be made since the material with the best tensile behavior (Al) has the least efficiency in compression.

Perhaps more importantly, the present results provide a framework for suggesting ways to improve these materials for energy-absorption applications. The first requirement is to obtain foams with a more regular cell structure (accomplished in polymer foams by using a surfactant in the foaming process). Higher uniformity will directly result in an increase in energy absorption efficiency since this was correlated with repeatable collapse forces throughout the structure. Greater uniformity would also lead to an increase in flow stresses by eliminating the weakest points. Further significant increase in flow strength and thus energy absorbing capacity should occur with improvements in the fracture resistance of the as-cast materials, because in the strongest available foams, the collapse mechanism largely consists of local fracture rather than plastic deformation. Increased resistance to fracture would also aid in making the foams practical in bending or long-column compression applications, which are currently not feasible due to gross fractures.

ACKNOWLEDGMENTS

The authors are grateful to Drs. P. Beardmore and K. R. Kinsman for critical reviews of the manuscript and to C. J. Amberger for much technical assistance.

REFERENCES

1. H. A. Kuhn and C. L. Downey: *J. Eng. Materials and Technology, Trans. ASME*, 1973, vol. 95, pp. 41-46.
2. W. Thiele: *Metals Mater.*, 1972, vol. 6, no. 8, pp. 349-52.
3. E. A. Meinecke and R. C. Clark: *Mechanical Properties of Polymeric Foams*. Technomic, Westport, Conn., 1973.
4. K. C. Rusch: *J. Appl. Polym. Sci.*, 1970, vol. 14, pp. 1433-47.
5. K. C. Rusch: *J. Appl. Polym. Sci.*, 1969, vol. 13, pp. 2297-2311.
6. A. N. Gent and A. G. Thomas: *J. Appl. Polym. Sci.*, 1959, vol. 1, pp. 107-13.
7. J. M. Lederman: *J. Appl. Polym. Sci.*, 1971, vol. 15, pp. 693-703.
8. V. A. Matonis: *SPE J.*, 1964, vol. 20, pp. 1024-30.
9. R. Chan and M. Nakamura: *J. Cell. Plast.*, 1969, vol. 5, no. 2, pp. 112-18.
10. M. R. Patel and I. Finnie: *J. Mater.*, 1970, vol. 5, no. 4, pp. 909-32.
11. M. C. Shaw and T. Sata: *Int. J. Mech. Sci.*, 1968, vol. 8, pp. 469-78.
12. G. F. Bolling and R. H. Richman: *Phil. Mag.*, 1969, vol. 19, pp. 247-64.
13. W. L. Fink and D. W. Smith: *Trans. AIME*, 1937, vol. 126, pp. 162-67.
14. R. E. Stotchdopole and L. C. Rubens: *J. Cell. Plast.*, 1965, vol. 1, pp. 91-96.
15. C. E. Massonnet and M. A. Save: *Plastic Analysis and Design*, vol. 1, Blaisdell, New York, 1965.
16. S. P. Timoshenko and J. M. Gere: *Theory of Elastic Stability*, McGraw Hill, New York, 1961.